A spatiotemporal dynamic analyses approach for dockless bike-share system

Jie Song[a], Liye Zhang[a,*], Zheng Qin[a], Muhamad Azfar Ramli[a]

[a] *Institute of High Performance Computing, A*Star, Singapore, 138632*

Abstract

The landscape of cycling activities from a dockless bike-share system is dynamic over space and time. Decoding usage patterns from bike-share trips have been a highly charged area in the literature. Therefore, this study aims at developing an analytical approach to understanding the trip demands of bike-share and model the spatiotemporal dynamics of cycling flows. Under the proposed framework, global and local Moran's I indexes measure the spatial autocorrelation of cycling trips in different traffic zones, and community detection extracts the network structure of bike traffic. The developed approach is subsequently applied to the dockless bike-share system in Singapore. It is found that the spatial distribution of cycling trips shows a significant clustering pattern. Specifically, the global Moran's indexes of weekdays are larger than that of the weekends in the same time span and, moreover, the global Moran's indexes of peak hours are smaller than the off-peak hours on the same day. Several hotspots with the top high local Moran's I values are detected, which keep relatively stable during different times of the day on both weekdays and weekends. We also found that there existed a stable community structure of bike-share trips. In contrast, the average sizes of the top 15 communities on a weekday were statistically higher than those on the weekend, at a significance level of 0.01. The proposed modeling framework provides practice insights to bike fleet management, cycling path design, and other urban and transportation planning practices.

Keywords: Bike-share system, Spatial autocorrelation, Spatiotemporal dynamics, Community detection

1. Introduction

Bike-share has taken a prominent place in the debates on sustainable transportation. It has obtained widespread popularity in an abundance of municipalities because of various benefits: mitigating rush-hour congestion (Wang and Zhou, 2017), reducing car ownership (Fishman et al., 2014), lessening carbon emissions (Cao and Shen, 2019; Zhang and Mi, 2018), and doing a service to health (Mueller et al., 2015; Woodcock et al., 2014). Approximately 1,500 cities in the world

*Corresponding author

Email addresses: songjie@ihpc.a-star.edu.sg (Jie Song), zhangly@ihpc.a-star.edu.sg (Liye Zhang), qinz@ihpc.a-star.edu.sg (Zheng Qin), ramlimab@ihpc.a-star.edu.sg (Muhamad Azfar Ramli)

have deployed bike-share systems, with an enormous number of bikes, more than 18 million (Liu et al., 2018). Bike-share systems collect an ocean of data in the form of GPS records, information that dramatically benefits scientists in investigating human movements (Padgham, 2012; Jurdak, 2013), multi-modal public transit systems (Romero et al., 2015; Martin and Shaheen, 2014), and other human-environment interactions (Iseki and Tingstrom, 2014). The ubiquity of big data has contributed to a spike of relevant publications. The past few years have witnessed over 200 papers, and more than a third have emerged since 2017 (Si et al., 2019). Si et al. (2019) highlighted three promising research themes: systematic optimization, the economic effect of sharing, and the factors influencing bike-share usage. The spatiotemporal signature of cycling activities, therefore, becomes a highly charged topic among the research community of bike-share (see, for example, (Liu and Lin, 2019; Beecham et al., 2014; McKenzie, 2020)).

The dynamics of bike-share systems have been explored via numerous techniques ranging from regression (Shen et al., 2018; Zhu and Diao, 2019), dimension reduction (Xu et al., 2019), clustering (Du et al., 2019; Etienne and Latifa, 2014; Zhou, 2015), to graph theories (Borgnat et al., 2011; Zhou et al., 2019). Complex network approaches have extensive applications in bioinformatics (Mason and Verwoerd, 2007), social network (Kossinets and Watts, 2006), and mass transit (Lu, 2018). However, they were not adopted to learn bike-share systems until several years ago, and recent research was in two directions. The first one is to use complex network theories to predict demands for shared bikes (Lin et al., 2018; Zhang and Meng, 2019). For instance, Ram et al. (2016) conducted network analysis on the demands of bike stations in Fortaleza, Brazil, and built an online viewer that showed temporal changes in the demands. Adham and Bentley (2016) employed community detection to aid in their algorithm on bike redistribution in London, inferring that the model efficiency increased partly owing to an integrated network tool. Ferreira et al. (2016) modeled a system of shared bikes as a network and allocated bike stations in a case study in Brazil, verifying that the population had better access to shared bikes that were reallocated by the simulation. The other mainstream of inquiries was the uncovering of the network structures of cycling flows (Zhang et al., 2019), which is less prevalent than the first. For example, Austwick et al. (2013) compared the schemes of shared bikes in five cities via network centrality indicators and community detection tools. The authors insinuated that on an aggregated level, all these systems share highly comparable temporal patterns: the utilization of bike-share systems peaked during rush hours and flatted out during the non-rush ones. Saberi et al. (2018) found that the connectivity among bike stations rose, and cycling flows soared in London's bike-share system after a shutdown of the city's major transit hubs — via complex network theories. Some more recent research appeared in China, where the practice of the ideas of free-float bike-share prospered. For example, Wei et al. (2019) revealed a system's topology from Yixing, China, based on several network properties and the shortest path theory.

The research to date has tended to focus on station-based systems rather than dockless programs. Previous studies have focused more on describing the spatial distributions of cycling activities. However, how the spatial correlations of travel demand over time vary is not statistically demonstrated. Past efforts have inclined to analyze arrival and departure trips separately, but what is not yet clear is the spatiotemporal dynamics of the networks of cycling activities from a stationless system. As recommended by Austwick et al. (2013), the disaggregation of cycling trips into hour-based time slots could uncover a more dynamic picture of shared bike usage over an entire day, revealing more subtle patterns than the daily snapshots of bike traffic do. Thus, this study aims to develop an analytical approach to quantify the spatial-temporal dynamics of a dockless bike-share system. More specifically, this approach can quantify the spatial distribution of the cycling trip, the network structure of trip demand, and how they evolve during a day on both weekdays and weekends.

This work contributes to the literature in two aspects. First, in the proposed framework, we model bike-share activities as both arrival/departure trips and a network containing cycling flows. The framework is able to identify spatial dependence of the arrivals and departures in different areas over time, and delineate the inter-dependence of different locations via the linkages of bike-share flows. The approach's nucleus is an integration of two essential tools: the identification of spatial autocorrelation and community detection. Second, the developed workflow can serve as a decision-support tool that is appropriate for the analysis of similar bike-share programs. Traffic authorities and the bike-share industry can benefit from this study's findings. For instance, the proposed approach has pinpointed the clustering locations of bike-share demand in Singapore and detected top communities of bike-share flows that exhibit distinct characteristic on weekdays and weekends. These findings would help to ameliorate the current planning of bike-share facilities and the optimization of resources.

2. Methodology

This study proposes an approach to analyze the spatial-temporal dynamics of the bike-share system from the perspective of trip spatial patterns and linkage between traffic zones. Specifically, the global spatial pattern and local hotspots of the cycling trips are measured by the spatial autocorrelation models. The linkage between traffic zones is modeled by a spatial community detection model, which can find regions with more connections among cycling journeys inside and fewer outside. The framework of this approach is illustrated as follows.

2.1. Logic Framework

The workflow framework of the spatial-temporal analysis of cycling traffic is displayed in Figure 1. There are three major modules: data collection and preprocessing, spatial distribution analysis of trips, and spatial-temporal analysis.

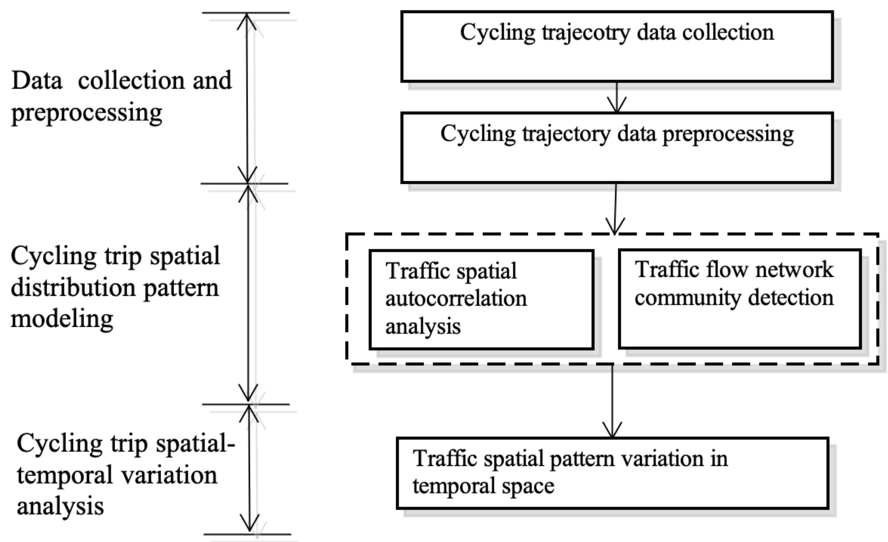

Figure 1: The logic framework of cycling traffic spatial-temporal analysis

Data collection and preprocessing. A major data preprocessing task for a bike-share data set is the elimination of data noise. The movement of shared bicycles are tracked by the Geographical Position System (GPS), which contain the information of the bicycle ID, trip index, pick up location and time stamp, drop off location and time stamp. The GPS can be occasionally flawed due to the errors in the process of data collection and reception. For example, there are trips with a very short duration, such as less than 2 minutes. Thus, GPS data must be refined to eliminate possible noise.

Traffic spatial distribution modeling. It contains two sub-modules: 1) the modeling of the spatial autocorrelation of cycling trips and 2) the community detection of traffic flows. The entire study area is divided into square traffic zones (TZ), which represent the origins and destinations of cycling flows. On top of the TZ configuration, we can build an origin-and-destination (OD) matrix. With the OD matrices, we are ready to model the spatial distribution of cycling traffic using the spatial autocorrelation model and network community detection model.

Spatial autocorrelation quantifies the variation of cycling flows in space. It involves two sub-components: spatial autocorrelation models on both global and local scales. The global one verifies overall whether there is a spatial clustering phenomenon of bike-share flows; the local model pin-points the hotpots exhibiting such patterns. The network community detection model is to identify regions with substantially more intra-region journey connections than inter-region counterparts. The community analysis is facilitated by a network layer overlaying with the square TZs. The purpose is to further understand the spatial distribution of bike-share trips from a network perspective to supplement and validate the spatial autocorrelation module. The mathematical formalities of the three modules will be introduced shortly.

Temporal variations of traffic spatial patterns. We can further study how the spatial configuration evolves. This qualitative investigation helps to demonstrate temporal variations of both autocorrelation and community network characteristics of a bike-share system.

2.2. Cycling flow graph and its features

2.2.1. Cycling flow graph

A dockless bike-share system can be represented by a directed graph, which can model the linkage among cycling flows in different regions. The graph is denoted as

$$G = \{V, E\} \tag{1}$$

where V is a set of the TZs, and E a set of edges. The TZs, land cells where bike-share journeys depart or arrive, are described by

$$V = \{TZ_i | TZ_i = i, 2, ...n\} \tag{2}$$

where n represents the number of TZs.

The edges in the network is denoted by

$$E = V \times V = \{e_{ij}\} \tag{3}$$

where e_{ij} is the edge between TZ_i and TZ_j. The GPS records have the journey information on different edges, which can be defined by:

$$T = \{C_m | C_m, m = 1, 2, \ldots, n\} \tag{4}$$

where C_m is journey m and n is the number of journeys. C_m can be express by

$$C_m = \{c_m^k | c_m^k = (t_k, x_m^{t^k}, y_m^{t^k})^T, k = 1, 2\} \tag{5}$$

where k is a time index, 1 origin or 2 destination, and c_m^k is the information vector of journey m at time t_k. It includes the geographic coordinates of journey m at time index t_k, x_m^k and y_m^k. The origin and destination coordinates of journey m are $(x_m^{t^1}, y_m^{t^1})$ and $(x_m^{t^2}, y_m^{t^2})$. If its coordinate $(x_m^{t^k}, y_m^{t^k})$ falls in zone TZ_i (Eq. 2), then it is denoted as $(x_m^{t^k}, y_m^{t^k}) \in TZ_i$.

Next, we can represent an OD matrix by

$$OD = \begin{bmatrix} od_{11} & od_{12} & \ldots & od_{1n} \\ od_{21} & \ddots & & od_{2n} \\ \vdots & & & \vdots \\ od_{n1} & od_{n2} & \ldots & od_{nn} \end{bmatrix} \tag{6}$$

where n denotes the number of TZs, od_{ij} is the number of journeys from TZ_i to TZ_j.

Furthermore, the set of the journeys between all OD pairs is expressed by $JN = \{JN_{i,j} | i = 1, 2, \ldots, n; j = 1, 2, \ldots, n\}$. Specifically, $JN_{i,j}$ represents the set of journeys from TZ_i to TZ_j, which is denoted by

$$JN_{i,j} = \{C_m | C_m \in C \wedge (x_m^{t^1}, y_m^{t^1}) \in TZ_i \wedge (x_m^{t^2}, y_m^{t_2^2}) \in TZ_j\} \tag{7}$$

The OD matrix is fundamental for the spatiotemporal analyses. For spatial autocorrelation analysis, it can be converted to two sets, one for arrival trips and the other for departure ones. The set of arrival trips is denoted by $A = \{A_i | A_i, i = 1, 2, \ldots, n\}$, and departure trips by $\{D_i | D_i, i = 1, 2, \ldots, n\}$, where n is the number of TZs. For community detection analyses, based on Eq. 3 and 6 the OD matrix is converted to a weight set $W = V \times V = \{w_{ij}\}$, where $w_{ij} = od_{ij} + od_{ji}$ is the final weight on the edge e_{ij}.

2.2.2. *Cycling graph features*

There exist network properties that describe the overall structure of a graph quantitatively. Centrality indicators, such as degree, are among the widely adopted measures. They offer a microscopic view of a network: for example, the locations of influential nodes that exerted attractive power on their neighboring ones and the presence of these nodes was critical to the stability of the whole graph.

Degree centrality relies on the assumption that a critical node has numerous direct connections with other nodes, with a high value of centrality accordingly. In a bike-share system, G, degree centrality of a TZ_i is represented by the number of immediate neighbors with which the TZ is connected. It was defined as

$$DC_{TZ_i} = deg(i) \tag{8}$$

where $deg(i)$ denotes the summation of the in-degree $indeg$ and out-degree $outdeg$ of a TZ i. And $indeg$ is the number of neighboring nodes that send trips to i, and $outdeg$ the neighboring nodes that received trips from i.

In practice, degree centrality is normalized to alleviate the impacts of nodes with extremely high or low values. The normalization enable the comparison of the distribution of degree centrality over a day. Normalized degree centrality NDC is computed by

$$NDC_{TZ_i} = \frac{DC_{TZ_i} - min(DC)}{max(DC) - min(DC)} \tag{9}$$

where DC_{TZ_i} is the degree centrality of a node i, $min(DC)$ and $max(DC)$ are the minimum and maximum values of a set DC that contains degree centrality of all nodes in the system.

2.3. *Spatial autocorrelation analysis*

Spatial autocorrelation analysis is a quantitative approach to assess the association of cycling activities over space. Two common indicators adopted by the spatial statistics community are employed: global and local Moran's I indexes.

2.3.1. Spatial weight matrix

A spatial weight matrix is constructed before we model the global and local spatial autocorrelation of bike-share trips. It is built upon a number of adjacent cells (square TZs mentioned earlier). The weight matrix of M cells is described by

$$W = [w_{i,j}]_{M\times M} = \begin{bmatrix} 0 & w_{12} & w_{13} & \dots & w_{1M} \\ w_{21} & 0 & w_{23} & \dots & w_{2M} \\ w_{31} & w_{32} & 0 & \dots & w_{3M} \\ \vdots & \vdots & \vdots & \ddots & \vdots \\ w_{M1} & w_{M2} & w_{M3} & \dots & 0 \end{bmatrix} \tag{10}$$

where i and j denote the cell number, the weight is defined by $w_{ij} = 1/d_{ij}$, and d_{ij} represents the Euclidean distance between the centroid of cell i and j, respectively.

2.3.2. The modeling of global autocorrelation

We are given a set of arrival or departure trips within a time interval and their geographic locations; spatial autocorrelation modeling aims at determining if the trips are clustered, dispersed, or systematically random. These hypotheses are verified by global Moran's I index. It can be computed by

$$I = \frac{\sum_{i=1}^{n} \sum\limits_{j=1}^{n} W_{ij} \times (x_i - \bar{x})(x_j - \bar{x})}{\rho^2 \sum_{i=1}^{n} \sum_{j=1}^{n} w_{ij}} \tag{11}$$

where x_i is the cycling trip volume of traffic zone i and $\bar{x}$ is the average trip volume of all traffic zones, ρ^2 is the variance of cycling trip of all traffic zones, and w_{ij} the spatial weight between cell i and j. It should be noted that the cycling trip of traffic zone x_i is the summary of the cycling trip leaving traffic zone i and the trips entering traffic zone i.

Moran's I ranges from -1 to 1, where a higher value greater than zero indicates a positive correlation among the observations over space, and a negative number suggests a spatially dispersed pattern.

2.3.3. The modeling of local autocorrelation

Local autocorelation modeling is demonstrated by local Moran's I indexes. An index is computed for every cell in a study area, reflecting potential hotpots seeing large number of departing or arriving trips in neighboring cells. It is calculated by

$$I_i = \frac{(n-1)(x_i - \bar{x}) \sum_{j=1}^{n} w_{ij} \times (x_j - \bar{x})}{\sum_{j=1, j\neq i}^{n} (x_j - \bar{x})^2} \tag{12}$$

where I_i is the Moran's I index of traffic zone i, x_i and x_j represent the cycling trip of traffic zone i and j, respectively, and $\bar{x}$ and w_{ij} are the same variables as defined by Eq. 11.

Local Moran's I does not have a [-1, 1] boundary, but it has a similar interpretation as does its global counterpart: a positive number point to a high-high relationship between neighbors and an index less than zero hints at a negative direction. For example, if there are two immediate cells with similar positive local Moran's I indexes, meaning that the large number of cycling trips in one cell is positively associated with that in the other cell.

2.4. The modeling of community structure

2.4.1. Community detection

Community detection categorizes relevant nodes into subgroups with high intra-flows and low inter-traffic volumes. There are three standard detection algorithms. Divisive algorithms cut off inter-group edges to classify communities, the agglomerative depends on a recursive process to label similar nodes with the same identification number, and optimization approaches treat the tasks as the solutions of objective functions (Blondel et al., 2008). While different algorithms follow their procedures, an essential logic remains identical: the methods all aim at amplifying the modularity of a network. The maximization of modularity, therefore, was an approach utilized by this study. For a bike-share system, the modularity is computed as

$$MOD = \frac{1}{2m} \sum_{i,j} \left(f_{ij} - \frac{O_i O_j}{2m} \right) \theta(c_i, c_j) \tag{13}$$
$$m = 1/2 \sum_{ij} f_{ij}$$

where f_{ij} is the trip volumes between TZs i and j, O_i and O_j are the cycling trips departing from i and j respectively, and $\theta(c_i, c_j)$ denoted a community multiplier with c_i and c_j being community labels of i and j, and with a value of 1 if $c_i = c_j$ or 0 if otherwise.

Louvain algorithm is employed by this work to detect sub-regions of cycling flows. Highly efficient, it is a fast greedy optimizer (Blondel et al., 2008) and has been proved valid in such network studies as docked public bikes (Austwick et al., 2013), and dockless schemes (Yang et al., 2019). This approach is capable of disclosing the internal community structure of large-scale networks such as bike-share systems, and it generates unsupervised outcomes. Louvain algorithm undertakes two iterative phases. The first phase involves the assignment of each node to a community, and consequently, the node quantity is the number of communities. Next, a node i is removed from its current community and joins the one to which its neighboring node j belongs. This rearrangement of community labels is to compute the increase of network-level modularity. Specifically, the node j's community gains the highest modularity increment by absorbing the node i. Mathematically, the gain of a community C with the new member of an isolated node i can be calculated by

$$\Delta Q = \left[\frac{\sum_{in} + 2K_{i,in}}{2m} - \left(\frac{\sum_{tot} + K_i}{2m}\right)^2\right] - \left[\frac{\sum_{in}}{2m} - \left(\frac{\sum_{tot}}{2m}\right)^2 - \left(\frac{K_i}{2m}\right)^2\right] \tag{14}$$

where $\sum_{in}$ is the sum of the weights (trip volumes in a bikesharing network) of all edges within C, $\sum_{tot}$ represents that of the weights of those links incident to nodes in C, K_i denotes the total weights of links incident to node i, $K_{i,in}$ the sum of weights of the edges originating from i to nodes in C, and m the total of all links' weights of a network.

The second phase of the Louvain algorithm is the reconstruction of a new network with nodes being the communities detected in the first step. The weights of those links between these nodes become the inputs to equation 14, which is a reiteration of the first phase, and the objective is to enhance network modularity by merging communities. The algorithm stops when either of the following two conditions satisfies. The modularity remains constant, or there is a peak point of the modularity.

3. Case study results

3.1. Data processing and descriptive statistics

The proposed method was carried out using the bike-share program in Singapore (Figure 3), a city-state located in southeastern Asia. Singapore is an appropriate case study for this study because of a few points. First, it is an island with one of the densest populations around the world, but its land area is tiny compared with other countries. Constrained land resources force the government to inhabit automobile-oriented development. Thus, the Singaporean authority steps up efforts to advocate public transit and active mobility modes. As early as Feb. 2017, a dockless bike-share system was introduced into the nation (Shen et al., 2018) and subsequently welcomed by both governmental agencies and riders. Another consideration was pertinent to the availability and quality of cycling data. Our empirical data contained records from all service providers and covered eight days continuously — spanning a public holiday, weekdays, and weekends, which facilitated the comparison of usage patterns horizontally.

We obtained the GPS points tracking the movements of all shared bikes in Singapore from January 1st to 8th, 2019, and eliminated data noise via several steps. The first check is to filter out abnormal movements. Journeys that are shorter than 100 m were flagged and excluded and those trips with a duration of more than 1 hour were considered invalid. The first pre-processing criterion is suggested by Xu et al. (2019) and Shen et al. (2018), who observed similar data errors when dealing with bike sharing data in Singapore. The second data engineering is to validate a sensible travel speed range of included cycling trips. The maximum speed of a bike on roads must not exceed 25 km/h, according to Land Transport Authority, Singapore. It is uncommon to see trips with an average speed greater than 30 km per hour, and thus these noise data points were discarded. The pre-processing of a bike-share data set can be implemented using the Pandas library on the Python platform. After the data pre-processing algorithm was implemented, the final dataset was generated, and the trips were cut into smaller data sets, each of which is in a 15-minute time slice.

Figure 2 shows the descriptive statistics of the usage of the bike-share system. Figure 2a indicates two peaks of the trip rates at around 7 am and 6 pm, suggesting that the bike-sharing may be a first and last mile solution for many commuters. On average, more riders appear during non-peak hours on weekends than on weekdays. This difference is intuitively understandable. On weekends, travel demands for work-related journeys may decline with a rise in leisure-related trips. The enclosed areas between the red and green lines in Figure 2a demonstrate that there is a shifted portion of the travel demands from peak to non-peak hours on weekends. Figure 2b and c display the distributions of the Euclidean distances and travel times of bike-share trips. Nearly all trips are within 5,000 m, and a large proportion of them fall below 1,000 m. The distribution of travel times is skewed right, and 5 minutes appear to have the highest probability both on weekdays and weekends. The distribution statistics imply that the examined bike-share system may be a short-distance transportation mode.

3.2. OD analysis of cycling trips

A 300*300 m grid was overlaid onto the case study area, and each was denoted as a TZ. This cell size was determined on grounds of two considerations. First, Some of recent studies on dockless bike-sharing systems have employed a grid cell size from 150 m to 500 m, and two case studies in Singapore adopted the sizes of 300 and 500 m (Yang et al., 2019; Xu et al., 2019; Shen et al., 2018). Yang et al. (2019) also stated that appropriate cell sizes help to capture the flows among traffic analysis zones. While oversized cells diminish traffic flows, small cells may lead to a greater variability of the results of statistical tests (Section 4.2). Second, the average OD distance in our data set is 900 m, with a median distance of 646 m. Over 80 percentage of the trips has a Euclidean distance greater than 300 m. Therefore, the selected cell size can ensure both the sufficient representation of inter-zonal flows and the adequacy of trips in a cell. Next, the OD estimation modeling described in Section 2.2.1 was applied. We obtained OD matrices by a 15-minute time period and arrival/departure trips for each TZ and then aggregated them into seven-time slots represent different times for each day in the data set: (morning peak) 06:00 - 08:59, 09:00 - 10:59, 11:00 - 13:59, 14:00-16:59, (evening peak) 17:00-18:59, 19:00-21:59, 22:00-05:59.

Figure 4 shows an example of OD matrices for peak hours on weekdays and weekends using the proposed approach. The dark blue blues reflect the trips between two TZs, and thicker lines indicate higher traffic. Particularly thick links only exist among some TZs, and the trip demands of a considerable amount of TZs are zero. During morning peaks, more specifically, the flows associated with TZs near metro lines appear to be substantially higher than those elsewhere. Trip demands on weekends differ from weekday's conditions slightly. On weekends, the flows adjacent to the southern coastline are over-represented, which is absent in weekday's case. We also constructed

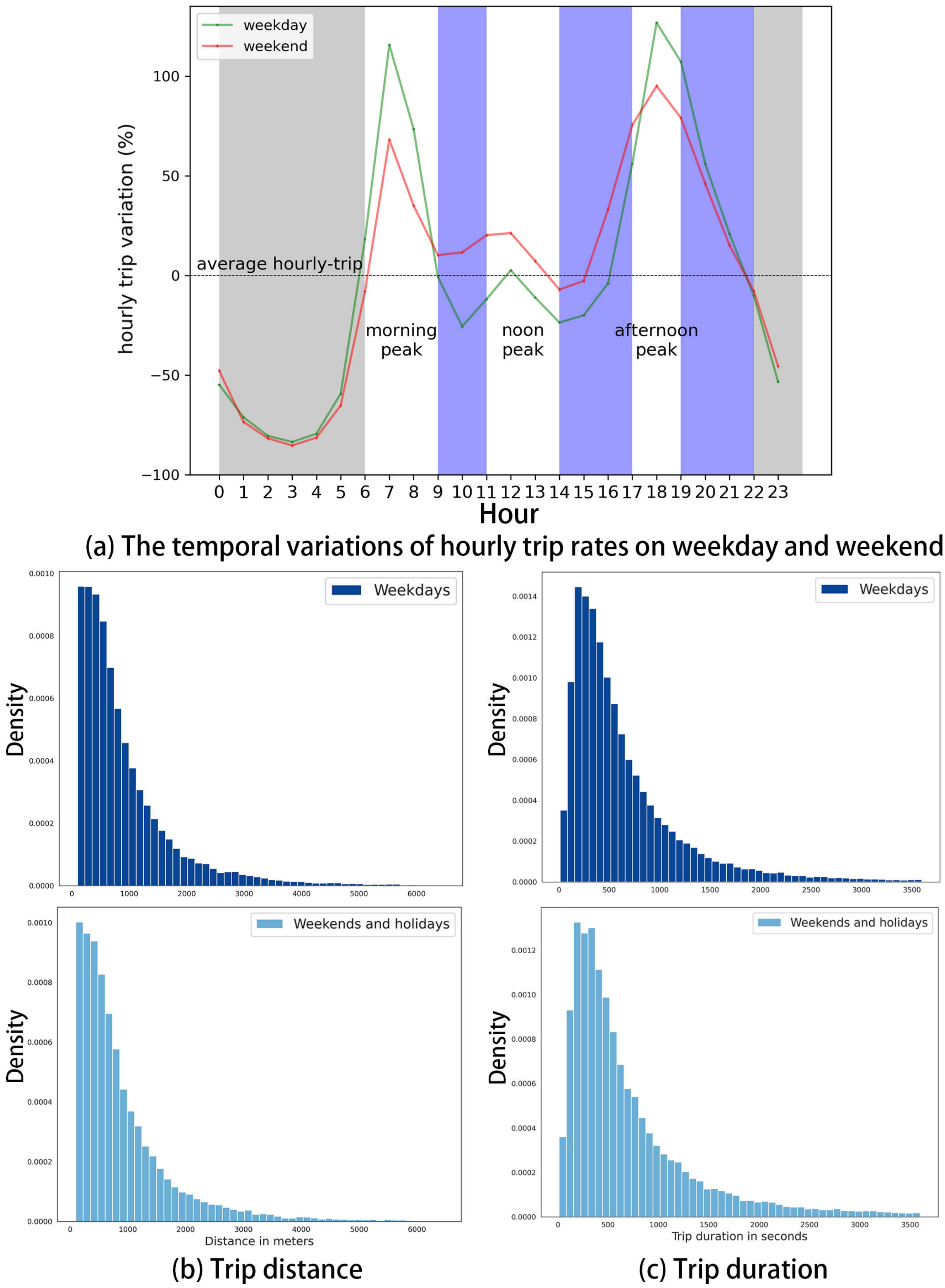

Figure 2: Descriptive statistics of cycling activities from the bike-share system

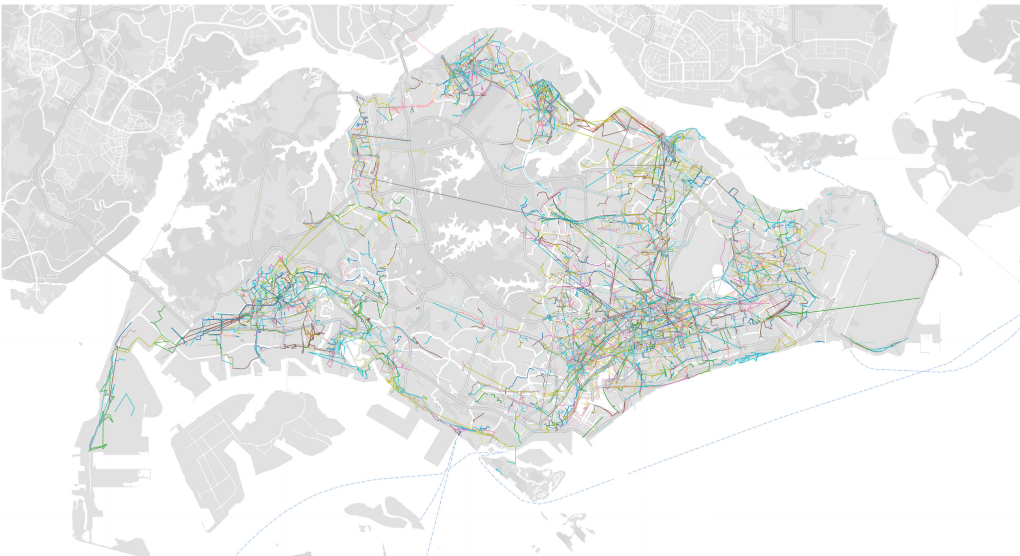

Figure 3: Study area showing cycling trajectories of its dockless bike-share system during morning peak on January 2, 2019

OD demand maps for off-peak hours on the other days and discovered that the OD matrices display a stable structure.

3.3. Spatiotemporal autocorrelation analysis

Table 1 shows the global Moran's I index of cycling trip distributions of 7 time spans both during weekdays and weekends. As aforementioned, the cycling trip volume of weekdays is the average volume from Monday to Friday, while the trip volume of weekends is the average volume from Saturday to Sunday. From Table 1, we can see that the cycling trip volume shows significant clustering patterns during all time spans of both weekdays and weekends, as implied by high Moran's Index values. Furthermore, the spatial distribution patterns of cycling trip on both weekday and weekend are largely similar, exhibiting a clustering tendency. Very interestingly, the global Moran's index of the morning peak and evening peak, marked in gray color in Table 1, are smaller than the other times spans. This means that the cycling trips during the peak hours seems less clustered compared with those during the non-peak hours.

Table 2 shows the top-10 local Moran's I index of cycling trip of TZs during weekday. The positive value of local Moran's I index indicates the TZs where the cycling trip volumes of the surrounding TZs are also high, which may be defined a cycling trip hotspot. Figure 5 shows the spatial distribution of the local Maran's I index. We can see that there are six significant cycling trip hotspots both in the morning peak and evening peak on weedays. We also checked the hotspots in the other time spans during both weekdays and weekends and found similar landscape. The hyperlocal clustering may be partly ascribed to land use conditions and connections to transportation nodes. Four hotspots lie in the center of peripheral residential towns such as Yishun (north) and Jurong East (West), and the other two are located in the downtown, filled with interchanges of

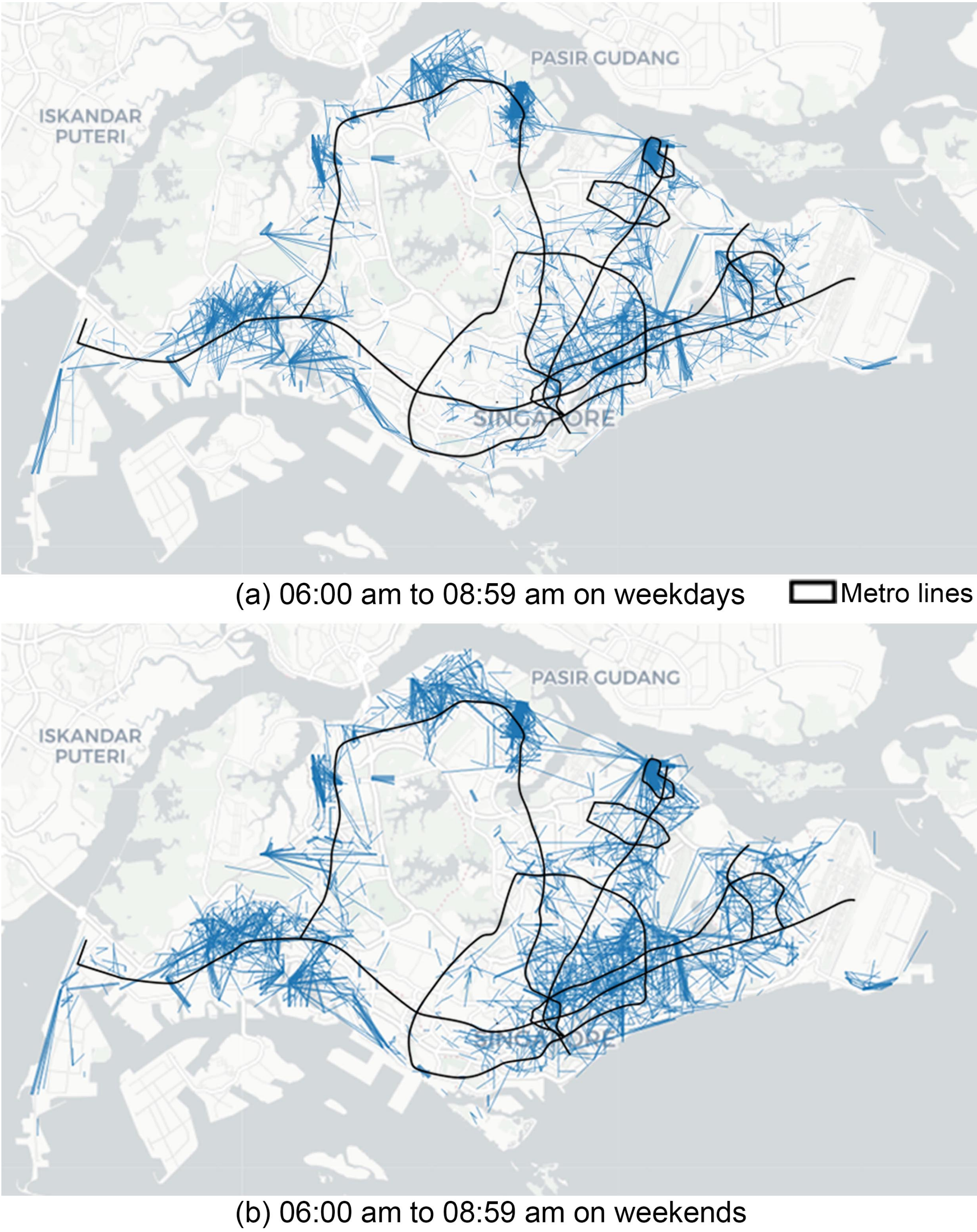

Figure 4: Bike-share flows among different OD pairs on weekday versus weekend

several subway lines. These six hotspots are quite stable temporally and maintain steady positions.

Table 1: Global Spatial Autocorrelation test

Day	No.	Time	Z-score	P-value	Moran's index	Spatial pattern
Weekday	1	06:00-08:59	71.379	$< 10^{-3}$	0.292	clustered
	2	09:00-10:59	108.881	$< 10^{-3}$	0.445	clustered
	3	11:00-13:59	121.781	$< 10^{-3}$	0.498	clustered
	4	14:00-16:59	118.587	$< 10^{-3}$	0.485	clustered
	5	17:00-18:59	105.978	$< 10^{-3}$	0.433	clustered
	6	19:00-21:59	110.971	$< 10^{-3}$	0.454	clustered
	7	22:00-05:59	127.182	$< 10^{-3}$	0.520	clustered
Weekend	1	06:00-08:59	49.549	$< 10^{-3}$	0.203	clustered
	2	09:00-10:59	91.100	$< 10^{-3}$	0.373	clustered
	3	11:00-13:59	105.384	$< 10^{-3}$	0.431	clustered
	4	14:00-16:59	94.601	$< 10^{-3}$	0.387	clustered
	5	17:00-18:59	89.045	$< 10^{-3}$	0.364	clustered
	6	19:00-21:59	96.230	$< 10^{-3}$	0.394	clustered
	7	22:00-05:59	107.755	$< 10^{-3}$	0.441	clustered

Table 2: Local Spatial Autocorrelation analysis (Weekday)

Day	No.	Zone ID	Cell Position	LM Index	Z-score	P-value
Morning peak	1	11632	(73,113)	203.389	12.542	0.001
	2	11472	(72,113)	182.217	23.972	0.001
	3	13211	(83,92)	128.806	9.013	0.002
	4	13051	(82,92)	105.939	23.511	0.001
	5	6828	(43,109)	76.204	10.734	0.002
	6	5386	(34,107)	68.561	22.360	0.001
Evening peak	1	12249	(77,90)	174.651	15.000	0.001
	2	12250	(77,91)	110.241	22.512	0.001
	3	7810	(49,131)	70.691	13.599	0.001
	4	12410	(78,91)	70.462	24.972	0.001
	5	7970	(50,131)	63.405	12.741	0.001
	6	5711	(36,112)	60.459	11.238	0.002

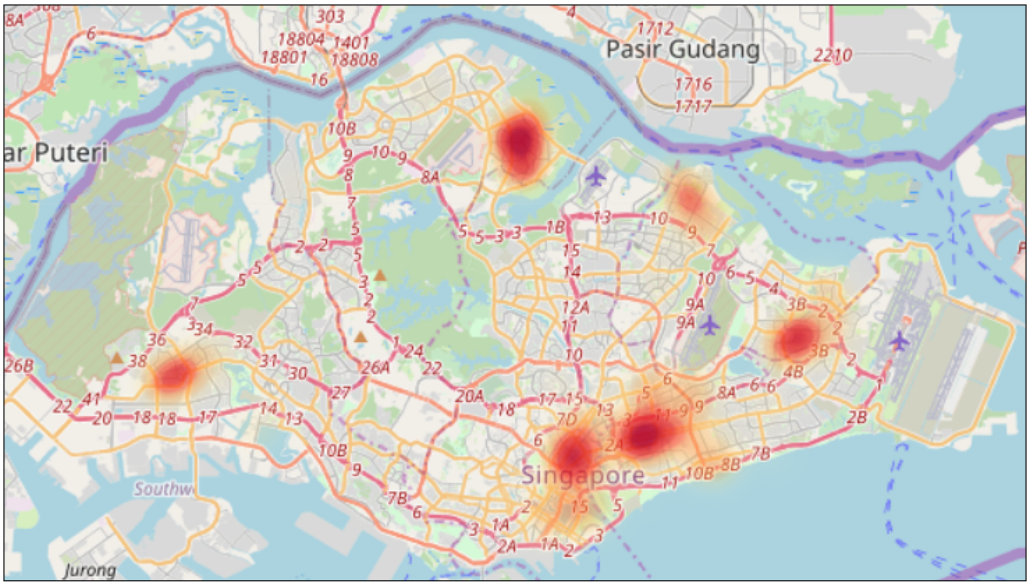

(a) Morning peak

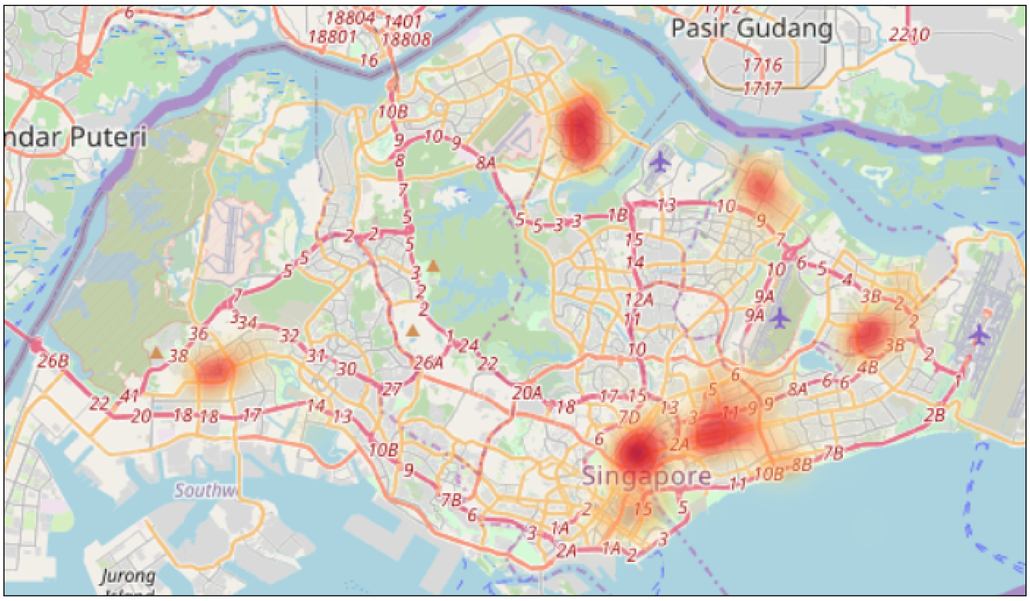

(b) Evening peak

Figure 5: The spatial distribution of Local Maron's I index on weekday

3.4. Spatio-tempopral community analysis

Figure 6 gives two snapshots of the community structures during morning and evening peak hours on weekdays. Both time slots witness a relatively stable composition of communities over the whole island: residential town, central business district, and scenic sites. OD pairs within a community are densely communicated via cycling flows.

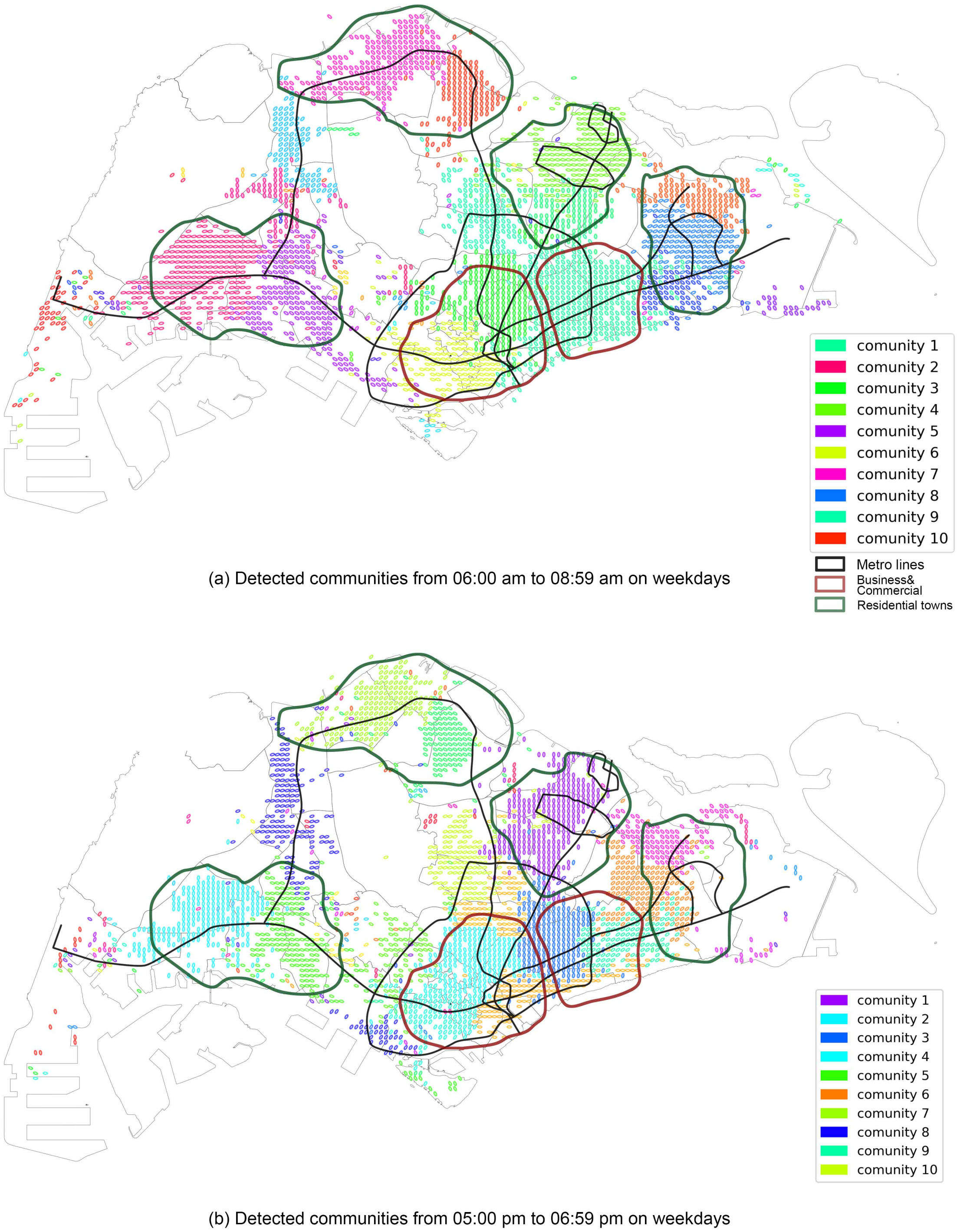

Figure 6: Community detection of bike-share trips during different times of weekday

Degree centrality of nodes suggest that communities on weekdays outstrip those on weekends in terms of important nodes with high degree centrality and average community size (Figure 7). There are discernible gaps between the polylines of weekday and weekend. The peak points of green lines indicate that the average value of the most critical nodes on weekdays exceeds 30, slightly doubling the number on weekends. During rush hours, these nodes are local hubs where a high volume of bike traffic goes through. Table 3 gives statistical evidence. It verifies the structural changes of the communities of cycling flows do occur temporally. At a significance level of 0.01, weekday's mean or median number of nodes in the top 15 communities is significantly higher than weekend's cases (Table 3). Based on our eight-day data set, it seems that bigger communities imply that on a work day, trip purposes may not be confined to the traditional notion of first-and-last-mile function of share bikes. End-to-end trips may take up a substantial portion of all journeys as longer travel distances become normal within communities of larger size and scale accordingly (but this is not substantiated by this study).

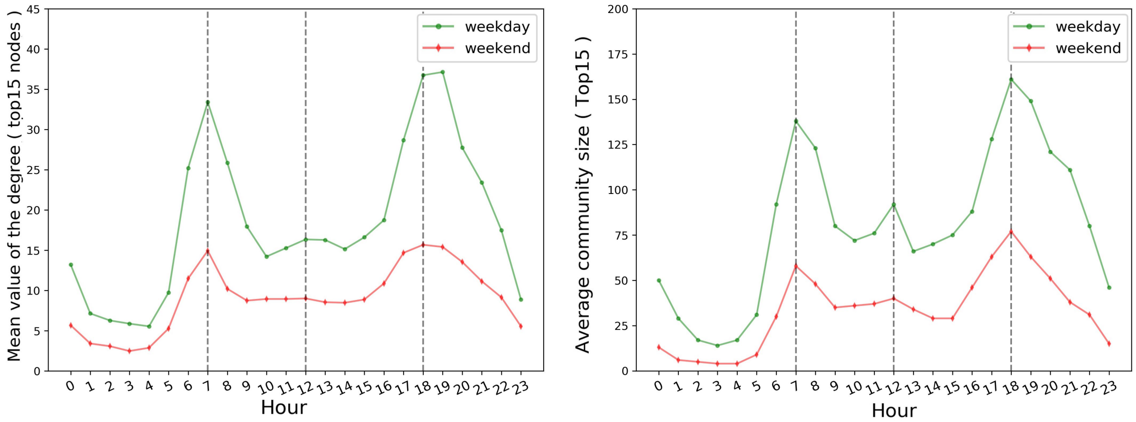

Figure 7: The evolution of network structure containing top 15 communities during a day. (left) The mean value of the degree centralities of nodes (right) The average community size defined as the number of nodes.

4. Discussions

4.1. Relationship among network properties, communities, and hotspots and their characteristics

There is a high level of consistency among the degree centrality, community detection, and local autocorrelation results. These measurements reveal a hierarchical structure of the spatial realization of cycling activities from a dockless bike-share system (for example, Figure showing an overlay). Degree centrality, as a network property, reflects globally those traffic zones that are critical to the entire network. Community detection further identifies the regions within which traffic zones are intensively interconnected, and bike traffic is centered on a few nodes with high degree centrality. These central nodes are labeled as local hotspots demonstrated by the local autocorrelation analysis. Moreover, the hotspots are located in relevant network communities.

Table 3: Hypothesis testings of the sizes of top 15 communities on weekdays versus weekends

Community ranked by the size of nodes	The mean or median number of nodes in the community (weekday)	The mean or median number of nodes in the community (weekend)	t score or W statistics	P-value
1	300*	179*	3.7467	0.0019
2	253*	143*	4.6284	0.0004
3	208**	122**	34.5**	0.0051
4	188**	112**	35**	0.0041
5	184**	110**	35.5**	0.0032
6	175*	110*	4.0344	0.0011
7	167*	106*	4.5495	0.0005
8	163*	99*	4.5139	0.0005
9	155*	97*	4.3583	0.0007
10	150*	87*	4.8340	0.0003
11	137*	82*	5.5251	0.0001
12	127*	70*	6.1110	0.0000
13	119*	66*	5.7486	0.0000
14	109*	62*	5.6853	0.0001
15	99*	56*	4.1409	0.0010

* denotes the mean. The samples passed both normality and equal-variance tests. Therefore, an unpaired two-sample t-test was employed with an alternative hypothesis $H_1 = \mu_{weekday} > \mu_{weekend}$: true difference in the means of the number of nodes in a community on weekdays and weekends is greater than zero.

** denotes the median. The samples were not normally distributed, so a non-parametric Wilcoxon test was used, generating a W statistics. The alternative hypothesis is $H_1 = median_{weekday} > median_{weekend}$: true difference in the medians of the number of nodes in a community on weekdays versus weekends is larger than zero.

Such a consistency validates the proposed approach in extracting a spatial structure from a dockless bike-share system.

Spatial clustering of bike-share ridership may be associated with specific land uses and critical transport nodes. For example, Figure 8 shows a local hotspot in Yishun, a northern rural town in Singapore, and appears to support the inference. Two land-use features embrace the hotspot. Two cores of the hotspot lie predominately in the immediate neighborhood of two metro stations, and the spatial extent of the hotspot overlays a residential district in the town. Such a phenomenon suggests an intriguing linkage between the spatial dynamics of bike-share trips and such contributing factors as land uses and the accessibility to critical transport nodes. Particularly, crucial public transit hubs (e.g., train stations and bus interchange) seem to attract the poles of a hotspot map. Thus, the interactions between public transit and bike-share will be a crucial line of investigation to learn better the usage of a shared system, which is a promising stream of research directions.

4.2. Biases and uncertainties of the outcomes

There are a few sources that may contribute to the biases of the results. First, spatial statistics always face the issues of the modifiable areal unit problem (MAUP). MAUP occurs when an analyst defines the spatial unit arbitrarily, which has been widely seen in landscape ecology, spatial health statistics, and other geography-related domains. MAUP definitely causes fluctuations in the outcomes, but researchers need to avoid deceptive results that may lead to unreliable conclusions. Hence, we conducted a sensitivity analysis on the hypothesis testing of global spatial autocorrelation of the departure trips on weekends. Figure 9 demonstrates that global spatial autocorrelation is statistically significant, in despite of varying grid cell sizes. However, smaller grid cell sizes appear to exhibit higher variations in Z scores, which means the testing outcome is somehow sensitive to small cell sizes. This is reasonable, because if a cell is too small, trips may spread uniformly. Figure 10 further demonstrates that departure trips exhibit a clustering tendency across all time spans, no matter which grid cell strategy is adopted. This observation is consistent with the statistics presented in Table 1. Although MAUP does not pose significant disturbance to the global testing outcomes, we expect it may vary the community structures and detected hotspots. Therefore, the resultant uncertainties of the findings should be anticipated, which must be interpreted with a grain of salt.

Second, the comparisons between the usage patterns of the system on weekdays and weekends need crucial annotations. The case study only employed an eight-day dataset, and thus the comparison on the aggregated level may not be statistically sufficiently. The number of daily maps on weekdays is larger than on weekends, resulting in the traffic densities on weekdays are higher than on weekends. Such inconsistency in the densities may lead to a gap between the data points representing the weekday and weekend case. Thus, the systematical biases within the resultant statistical comparisons must be acknowledged. The community structure on weekdays appear to be larger than on weekends, which may be ascribed to the fact that more data points represent

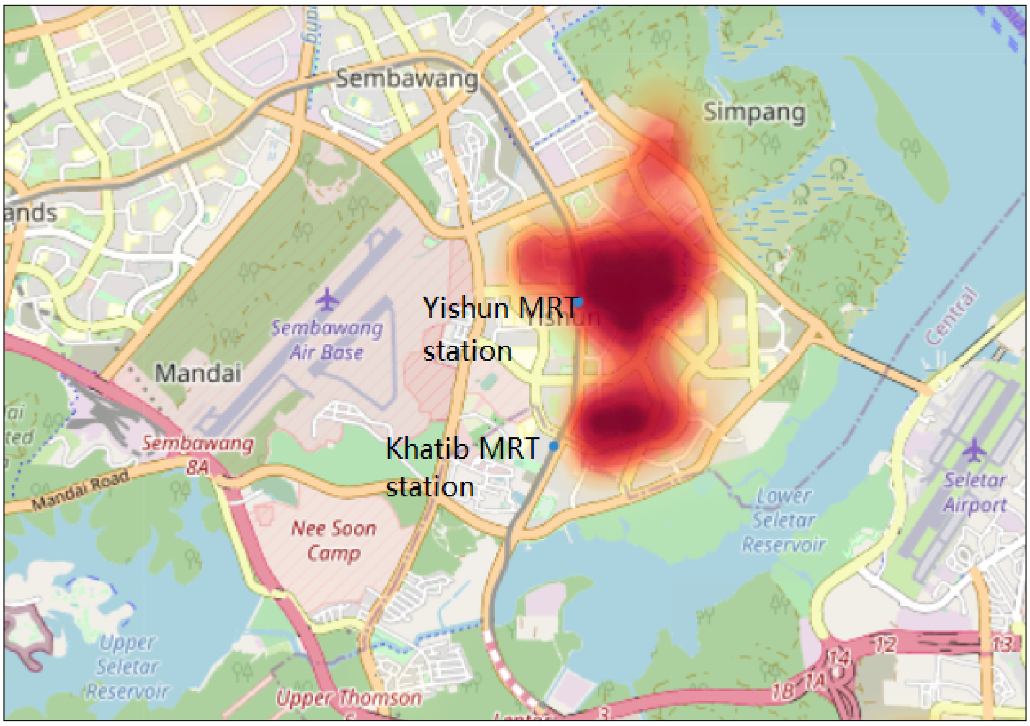

(a) Morning peak on Weekday

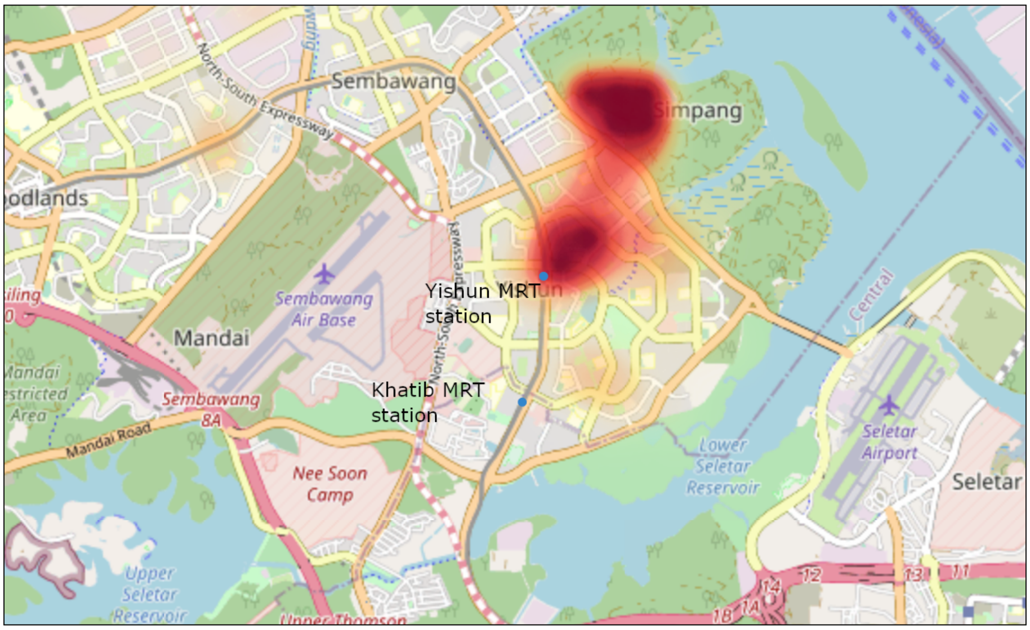

(b) Morning peak on Weekend

Figure 8: The spatial distribution of Local Maron's I index in Yishun area

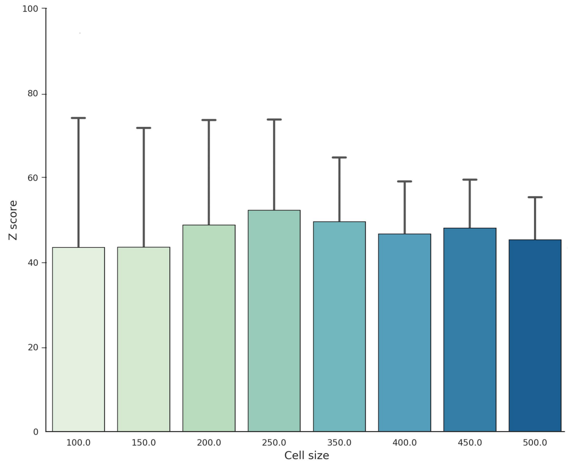

Figure 9: Z values of the global spatial autocorrelation tests of departure trips on weekdays by different grid cell sizes

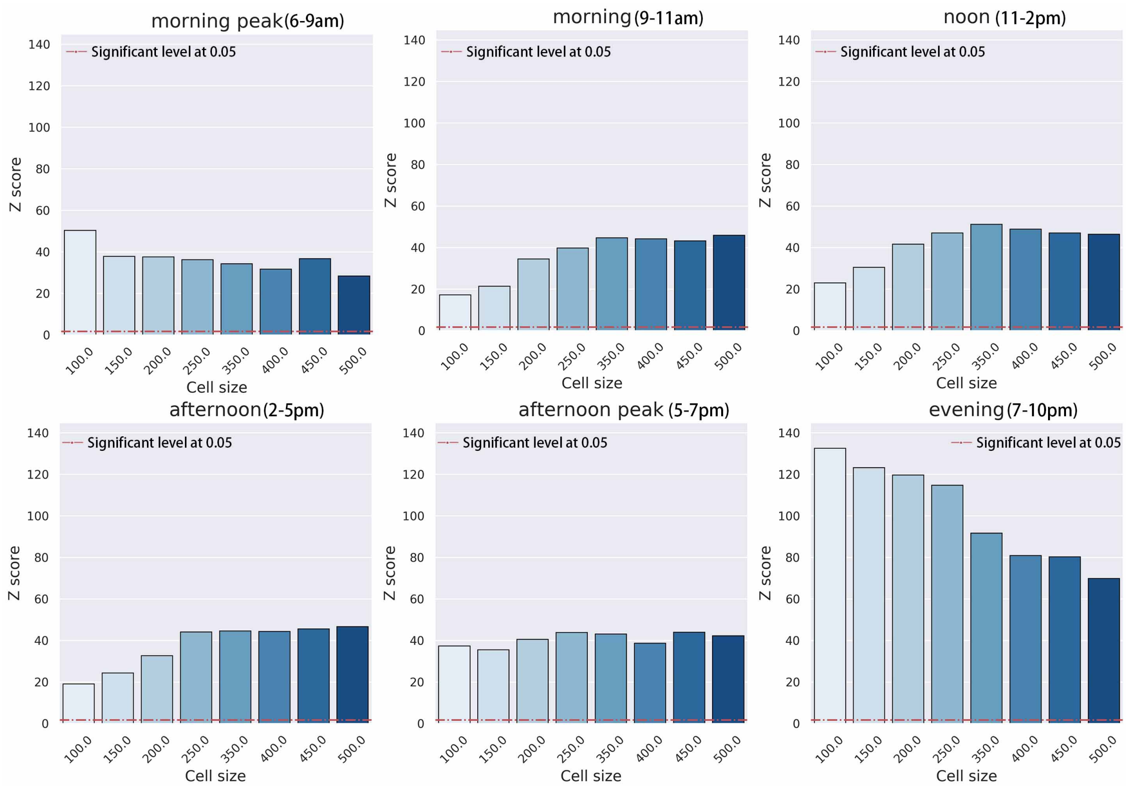

Figure 10: Z values of the global spatial autocorrelation tests of departure trips on weekdays by different grid cell sizes and periods

weekdays. Hence, the difference may not necessarily imply a behavioral distinction of usage patterns and trip purposes on weekdays and weekends. In other words, the difference may be amplified due to the data sparsity on weekends and the biased comparison.

4.3. potential applications of the framework

Bike-share operators may find this approach useful in allocating shared facilities. The analytical results hint at two pieces of information. First, they pinpoint at what times of a day there is spatial clustering of bike traffic and where the clusters are situated. Furthermore, the temporal analysis of the Moran's I indexes identifies traffic zones with consistently high values of local Moran's I index, which may be stable hotspots. Accordingly, resource managers should give these hotspots a higher priority when designing the scheduling of bicycle fleet deployment.

Urban planners can benefit from the proposed method as well. The community detection results have implications on the planning of new towns and urban redevelopment. A community of bike-share traffic is a prototype for a cycling-friendly town; inter-community linkages are ideal candidates of park connectors and city-wide cycling paths. A case in point is Singapore. One theme of the urban redevelopment planning for this island state is to extend the current network of cycling paths to nearly 1,000 km by 2026. Where to plug additional paths into the city needs to be pondered over. Conventionally planners administer surveys to cyclists and can understand their behaviors, but now the professionals can take advantage of big bike-share data. With the proposed approach, the planners of urban cycling can generate underlying insights from the data. Helpful information inferred by the approach includes the identification of stable hotspots and the community morphology of bike-share traffic. The stable hotspots are potential candidates for the nexuses of a cycling-path plan. Community morphology tells a different yet essential story: a cycling path network is unnecessarily identical to a road network that penetrates an entire city, and it can be zone-based. Zonal boundaries should be easily demarcated according to community detection outcomes. There is a cycling path network for each zone, and different zones are then linked through regional connectors. The routes of connectors partly depend on the locations of those stable hotspots. The end product will be a scheme for hierarchical cycling path network. It is another use case of the spatiotemporal analysis approach for a bike-share system, a tangible decision-support tool for urban planning practice.

5. Concluding remarks

This work proposed an analytical framework that aims at drawing insights from the spatiotemporal patterns of cycling activities from a given dockless bike-share system. It bolsters the decision making of the operation of bike-share systems and transportation planning. The framework contains three components: the pre-processing of bike-share data, the modeling of spatial traffic distribution, and the analysis of traffic spatiotemporal variations. The pre-process component instructs how to clean raw data in the form of cycling trajectories and estimate origin-and-destination demands for a series of time slots. The modeling of spatial traffic distribution includes two modules: spatial autocorrelation analysis based on the arrival and departure trips in traffic zones and community detection of bike-share flows among the zones. Spatial autocorrelation modeling depicts a complete picture of the space-time landscape of bike-share traffic. Community detection enriches the picture by analyzing cycling flow dynamics based on complex network theories.

The proposed approach is subsequently applied to the dockless bike-share system in Singapore. An eight-day bike-share data set was employed to evaluate the proposed framework. ~~It resulted in 109,458 valid trips, and~~ The data set was sliced into seven segments that correspond to peak and non-peak hours of a day. The results showed that the OD demands were spatiotemporally stable, with a large number of OD pairs seeing zero trips. It is found that the spatial distribution of the cycling trips shows significant clustering pattern.Specifically, the global Moran's indexes of weekdays are larger than that of the weekends in the same time span and, moreover, the global Moran's indexes of peak hours are smaller than the off-peak hours on the same day. Several hotspots with the top high local Moran's I values are detected, which keep relatively stable during different time of the day on both weekday and weekends. A similar story can be told of the community structure of bike-share trips as well. Overall, community boundaries were demarcated and robust. However, the scale of the top 15 biggest communities on weekdays is significantly larger than that on weekends, at a p-value of less than 0.01, suggesting temporal variations. However, the spatial communities of cycling activities either on weekdays or weekends remain stable across a day, and communities on weekdays have more complete shapes than their weekend counterparts based on the observations of the eight-day cycling trips. The findings and the proposed approach can support the decision making of bike-share operators and urban planners.

Acknowledgments

We thank the editor for handling this manuscript and thank the anonymous reviewers whose constructive comments helped us improve the draft significantly. This research is supported by the National Research Foundation, Prime Minister's Office, Singapore under its Urban Mobility Grant Challenge Program (Award No. UMGC-L005). The views expressed herein are those of the authors and are not necessarily those of the funding agencies.

References

Adham, M.T., Bentley, P.J., 2016. Evaluating clustering methods within the artificial ecosystem algorithm and their application to bike redistribution in london. Biosystems 146, 43 – 59. URL: `http://www.sciencedirect.com/science/article/pii/S0303264716300491`, doi:`https://doi.org/10.1016/j.biosystems.2016.04.008`. information Processing in Cells and Tissues.

Austwick, M.Z., O'Brien, O., Strano, E., Viana, M., 2013. The structure of spatial networks and communities in bicycle sharing systems. PloS one 8, e74685.

Beecham, R., Wood, J., Bowerman, A., 2014. Studying commuting behaviours using collaborative visual analytics. Computers, Environment and Urban Systems 47, 5 – 15. URL: http://www.sciencedirect.com/science/article/pii/S0198971513001014, doi:https://doi.org/10.1016/j.compenvurbsys.2013.10.007.

Blondel, V.D., Guillaume, J.L., Lambiotte, R., Lefebvre, E., 2008. Fast unfolding of communities in large networks. Journal of statistical mechanics: theory and experiment 2008, P10008.

Borgnat, P., Abry, P., Flandrin, P., Robardet, C., Rouquier, J.B., Fleury, E., 2011. Shared bicycles in a city: A signal processing and data analysis perspective. doi:10.1142/S0219525911002950.

Cao, Y., Shen, D., 2019. Contribution of shared bikes to carbon dioxide emission reduction and the economy in beijing. Sustainable Cities and Society 51, 101749. URL: http://www.sciencedirect.com/science/article/pii/S2210670719308765, doi:https://doi.org/10.1016/j.scs.2019.101749.

Du, Y., Deng, F., Liao, F., 2019. A model framework for discovering the spatio-temporal usage patterns of public free-floating bike-sharing system. Transportation Research Part C: Emerging Technologies 103, 39 – 55. URL: http://www.sciencedirect.com/science/article/pii/S0968090X18306673, doi:https://doi.org/10.1016/j.trc.2019.04.006.

Etienne, C., Latifa, O., 2014. Model-based count series clustering for bike sharing system usage mining: A case study with the vélib' system of Paris. ACM Transactions on Intelligent Systems and Technology 5. doi:10.1145/2560188.

Ferreira, F.A., Fonseca, C.S., Vital, D., Bastos-Filho, C.J., 2016. Assignment of shared bike stations based on network sciences. IEEE Latin America Transactions 14, 3957–3961.

Fishman, E., Washington, S., Haworth, N., 2014. Bike share's impact on car use: Evidence from the united states, great britain, and australia. Transportation Research Part D: Transport and Environment 31, 13 – 20. URL: http://www.sciencedirect.com/science/article/pii/S1361920914000480, doi:https://doi.org/10.1016/j.trd.2014.05.013.

Iseki, H., Tingstrom, M., 2014. A new approach for bikeshed analysis with consideration of topography, street connectivity, and energy consumption. Computers, Environment and Urban Systems 48, 166 – 177. URL: http://www.sciencedirect.com/science/article/pii/S0198971514000891, doi:https://doi.org/10.1016/j.compenvurbsys.2014.07.008.

Jurdak, R., 2013. The Impact of Cost and Network Topology on Urban Mobility: A Study of Public Bicycle Usage in 2 U.S. Cities. PLoS ONE 8, e79396. URL: https://dx.plos.org/10.1371/journal.pone.0079396, doi:10.1371/journal.pone.0079396.

Kossinets, G., Watts, D.J., 2006. Empirical analysis of an evolving social network. science 311, 88–90.

Lin, L., He, Z., Peeta, S., 2018. Predicting station-level hourly demand in a large-scale bike-sharing network: A graph convolutional neural network approach. Transportation Research Part C: Emerging Technologies 97, 258 – 276. URL: http://www.sciencedirect.com/science/article/pii/S0968090X18300974, doi:https://doi.org/10.1016/j.trc.2018.10.011.

Liu, H.C., Lin, J.J., 2019. Associations of built environments with spatiotemporal patterns of public bicycle use. Journal of Transport Geography 74, 299–312. doi:10.1016/j.jtrangeo.2018.12.010.

Liu, Y., Szeto, W., Ho, S.C., 2018. A static free-floating bike repositioning problem with multiple heterogeneous vehicles, multiple depots, and multiple visits. Transportation Research Part C: Emerging Technologies 92, 208 – 242. URL: http://www.sciencedirect.com/science/article/pii/S0968090X18301761, doi:https://doi.org/10.1016/j.trc.2018.02.008.

Lu, Q.C., 2018. Modeling network resilience of rail transit under operational incidents. Transportation Research Part A: Policy and Practice 117, 227 – 237. URL: http://www.sciencedirect.com/science/article/pii/S0965856417310716, doi:https://doi.org/10.1016/j.tra.2018.08.015.

Martin, E.W., Shaheen, S.A., 2014. Evaluating public transit modal shift dynamics in response to bikesharing: a tale of two u.s. cities. Journal of Transport Geography 41, 315 – 324. URL: http://www.sciencedirect.com/science/article/pii/S0966692314001409, doi:https://doi.org/10.1016/j.jtrangeo.2014.06.026.

Mason, O., Verwoerd, M., 2007. Graph theory and networks in biology. IET systems biology 1, 89–119.

McKenzie, G., 2020. Urban mobility in the sharing economy: A spatiotemporal comparison of shared mobility services. Computers, Environment and Urban Systems 79, 101418. URL: http://www.sciencedirect.com/science/article/pii/S0198971519303060, doi:https://doi.org/10.1016/j.compenvurbsys.2019.101418.

Mueller, N., Rojas-Rueda, D., Cole-Hunter, T., de Nazelle, A., Dons, E., Gerike, R., Götschi, T., Panis, L.I., Kahlmeier, S., Nieuwenhuijsen, M., 2015. Health impact assessment of active transportation: A systematic review. Preventive Medicine 76, 103 – 114. URL: http://www.sciencedirect.com/science/article/pii/S0091743515001164, doi:https://doi.org/10.1016/j.ypmed.2015.04.010.

Padgham, M., 2012. Human movement is both diffusive and directed. PloS one 7, e37754.

Ram, S., Dong, F., Currim, F., Wang, Y., Dantas, E., Sabóia, L.A., 2016. Smartbike: Policy making and decision support for bike share systems, in: 2016 IEEE International Smart Cities Conference (ISC2), IEEE. pp. 1–6.

Romero, J.P., Moura, J.L., Ibeas, A., Alonso, B., 2015. A simulation tool for bicycle sharing systems in multimodal networks. Transportation Planning and Technology 38, 646–663. URL: https://doi.org/10.1080/03081060.2015.1048946, doi:10.1080/03081060.2015.1048946, arXiv:https://doi.org/10.1080/03081060.2015.1048946.

Saberi, M., Ghamami, M., Gu, Y., Shojaei, M.H.S., Fishman, E., 2018. Understanding the impacts of a public transit disruption on bicycle sharing mobility patterns: A case of tube strike in london. Journal of Transport Geography 66, 154 – 166. URL: http://www.sciencedirect.com/science/article/pii/S0966692317302247, doi:https://doi.org/10.1016/j.jtrangeo.2017.11.018.

Shen, Y., Zhang, X., Zhao, J., 2018. Understanding the usage of dockless bike sharing in singapore. International Journal of Sustainable Transportation 12, 686–700. URL: https://doi.org/10.1080/15568318.2018.1429696, doi:10.1080/15568318.2018.1429696, arXiv:https://doi.org/10.1080/15568318.2018.1429696.

Si, H., gang Shi, J., Wu, G., Chen, J., Zhao, X., 2019. Mapping the bike sharing research published from 2010 to 2018: A scientometric review. Journal of Cleaner Production 213, 415 – 427. URL: http://www.sciencedirect.com/science/article/pii/S0959652618338678, doi:https://doi.org/10.1016/j.jclepro.2018.12.157.

Wang, M., Zhou, X., 2017. Bike-sharing systems and congestion: Evidence from us cities. Journal of Transport Geography 65, 147 – 154. URL: http://www.sciencedirect.com/science/article/pii/S0966692317302715, doi:https://doi.org/10.1016/j.jtrangeo.2017.10.022.

Wei, S., Xu, J., Ma, H., 2019. Exploring public bicycle network structure based on complex network theory and shortest path analysis: the public bicycle system in yixing, china. Transportation Planning and Technology 42, 293–307. URL: https://doi.org/10.1080/03081060.2019.1576385, doi:10.1080/03081060.2019.1576385, arXiv:https://doi.org/10.1080/03081060.2019.1576385.

Woodcock, J., Tainio, M., Cheshire, J., O'Brien, O., Goodman, A., 2014. Health effects of the London bicycle sharing system: Health impact modelling study. BMJ (Online) 348. doi:10.1136/bmj.g425.

Xu, Y., Chen, D., Zhang, X., Tu, W., Chen, Y., Shen, Y., Ratti, C., 2019. Unravel the landscape and pulses of cycling activities from a dockless bike-sharing system. Computers, Environment and Urban Systems 75, 184 – 203. URL: http://www.sciencedirect.com/science/article/pii/S0198971518305192, doi:https://doi.org/10.1016/j.compenvurbsys.2019.02.002.

Yang, Y., Heppenstall, A., Turner, A., Comber, A., 2019. A spatiotemporal and graph-based analysis of dockless bike sharing patterns to understand urban flows over the last mile. Computers, Environment and Urban Systems 77, 101361. URL: https://www.sciencedirect.com/science/article/pii/S0198971519301516, doi:10.1016/J.COMPENVURBSYS.2019.101361.

Zhang, J., Meng, M., 2019. Bike allocation strategies in a competitive dockless bike sharing market. Journal of Cleaner Production 233, 869 – 879. URL: http://www.sciencedirect.com/science/article/pii/S0959652619320232, doi:https://doi.org/10.1016/j.jclepro.2019.06.070.

Zhang, W., Tian, Z., Zhang, G., Dong, G., 2019. Spatial-temporal characteristics of green travel behavior based on vector perspective. Journal of Cleaner Production 234, 549 – 558. URL: http://www.sciencedirect.com/science/article/pii/S0959652619320864, doi:https://doi.org/10.1016/j.jclepro.2019.06.132.

Zhang, Y., Mi, Z., 2018. Environmental benefits of bike sharing: A big data-based analysis. Applied Energy 220, 296 – 301. URL: http://www.sciencedirect.com/science/article/pii/S0306261918304392, doi:https://doi.org/10.1016/j.apenergy.2018.03.101.

Zhou, X., 2015. Understanding spatiotemporal patterns of biking behavior by analyzing massive bike sharing data in Chicago. PLoS ONE 10. doi:10.1371/journal.pone.0137922.

Zhou, Y., Li, Y., Zhu, Q., Chen, F., Shao, J., Luo, Y., Zhang, Y., Zhang, P., Yang, W., 2019. A reliable traffic prediction approach for bike-sharing system by exploiting rich information with temporal link prediction strategy. Transactions in GIS 23, 1125–1151. URL: https://onlinelibrary.wiley.com/doi/abs/10.1111/tgis.12560, doi:10.1111/tgis.12560.

Zhu, Y., Diao, M., 2019. Understanding the spatiotemporal patterns of public bicycle usage: A case study of hangzhou, china. International Journal of Sustainable Transportation 0, 1–14. URL: https://doi.org/10.1080/15568318.2018.1538400, doi:10.1080/15568318.2018.1538400, arXiv:https://doi.org/10.1080/15568318.2018.1538400.